Time Resolved Pulsed Photoacoustic Spectroscopy of Formaldehyde Molecules at 266 nm

F. Yehya[1] , A. K. Chaudhary[2] , Konda[2]. S , &, Rasel .A.A. Mukred[3]

[1]Department of Physic, Faculty of Education & Sciences , Albaydha University, Albaydha , Yemen
[2]Advanced Centre of Research in High Energy Materials, University of Hyderabad, Hyderabad-500 046, India
[4]Department of Chemistry , Faculty of Education & Sciences , Albaydha University, Albaydha , Yemen
[1]fahembajash@gmail.com & [2]anilphys@yahoo.com

DOI: https://doi.org/10.56807/buj.v2i3.113

Abstract

We have reported the time resolved pulsed Photoacoustic (PA) spectrum of formaldehyde molecules (CH_2O). We have employed special designed PA resonance (L =27cm, R =1.4 cm) coupled with special filter. The 4^{th} harmonic i.e. 266nm (UV) pulses obtained from Q-switched Nd: YAG laser having 7 ns pulse width is used to excite the resonant modes of the cavity. Photoacoustic spectrum of formaldehyde is recorded in time and frequency domains. In addition, we have studied other important factors such as minimum detection limit, incident laser energy, effect of sample pressure, Acquiescing time and the efficiency of PA cells with different excited modes.

Keywords: *Photoacoustic, formaldehyde, Nd:YAG laser.*

دراسة طيفية لجزيئات الفورمالديهيد عند طول موجي 266نانومتر باستخدام التقنية الضوء-صوتية المعتمدة على الليزر النبضي

ملخص

في هذا البحث قمنا بدراسة طيفية لجزيئات الفورمالديهيد باستخدام التقنية الضوء-صوتية المعتمدة على الليزر النبضي. حيث صممنا خلية اسطوانية صوتية رنانة طولها 27سم ونصف قطرها 1.4 سم متصلة بمرشح خاص .كما قمنا باستخدام ليزر من نوع الياج - نادميوم مفتاح كيو - نبضي عرض النبضة 7نانومتر وذلك لإثارة الأنماط الرنانة للخلية الصوتية .طيف الفورمالديهيد تم قياسه وتسجيله في النطاقين الزمني والترددي. بالإضافة الى ذلك قمنا بدراسة تأثير كل من ضغط العينة وطاقة الليزر على الإشارة الضوء-صوتية. أخير تم حساب أقل قيمة ممكنة لقياس نسبة الفورمالديهيد.

كلمات مفتاحية: *ضوء-صوتية, فورمالديهيد, ليزر الياج - نادميوم.*

1. Introduction

Photoacoustic spectroscopy is one of the most popular and efficient absorption technique which is mainly used to detect different types of atmospheric pollutants at trace level *(Sigrist, (1994&2001) Miklós, (2001))* In Photoacoustic (PA) technique, the molecular samples absorb the photons which results in the excitation of molecular energy level. The excited state released its energy either by radiative or non-radiative processes (collisional relaxation). As the radiative lifetime of vibrational level are longer than the time required for collisional deactivation; therefore, the absorbed energy is completely released in the form of heat. Due to advance of laser technology and sensitivity of

microphones, the present form of photoacoustic spectroscopy becomes one of the most efficient and versatile tool to study the non-radiative relaxation transition in solid, liquid and gas samples. *(Sigrist, (1994&2001) Miklós, (2001) Slezak, (2003) Harren, (2000) Schäfer (1998) Yehya, (2011, 2013&2014) Kond (2014&2017))*

Formaldehyde (H_2CO) is a colorless gas and one of the most dangerous toxins that can be found in living space. Therefore, formaldehyde gas is responsible for serious problems of indoor air quality for several years *(Angelmahr, (2006))*. Formaldehyde, also known as methanal, methyl aldehyde and methylene oxide, is the first member of the aldehyde chemical family. *(Davenport , January 2014)*

Formaldehyde is known due to its highly toxic, impact on air quality and is one of the precursors of ozone and peroxyacetyl nitrates (PAN) *(Brasseur ,(1999)).* Vehicle exhaust and fugitive industrial emissions are considered as a primary H_2CO sources, while secondary H_2CO is produced mainly from the breakdown of primary volatile organic compounds (VOCs) via photochemical oxidation . Formaldehyde is allergenic, a potential human carcinogen and has high contribution into a pollutant in atmosphere. It can reach concentration levels in excess of 40 parts per billion (ppb) in polluted, urban environments *(Adewuyi, (1984), Anderson (1996) Hak (2005))*

H_2CO is considered as one of the most serious indoor contaminating trace gases present in new homes. It has been emitted from cheap chipboards, clothes, dyes and carpets. The World Health Organization (WHO) specified that the concentration of H2CO in residential indoor areas must not exceed 82 ppb for 30 min *(Ebeler (1997)))* Formaldehyde is also a valuable industrial chemical with limited alternatives *(Lu Y, (2010) Kim (2010) Nielsen (2010)).*

At various pressures and temperatures, the spectral absorption of formaldehyde near-UV measurements can be divided into two parts:

The first part is the formaldehyde vibronic system (˜A1A2 ← ˜X1A1) in the region of (38450 cm−1 - 27390 cm−1) (260 nm -365 nm). The second part is the partially rotationally resolved 4_0^1 rovibronic band in the region (28140 cm−1- 28330 cm−1) (355.20 nm - 352.90nm). In 1934,at low temperature, Dieke and Kistiakowsky reported the rovibronic fine structure of the 4_0^1 band absorption spectrum to evaluate the rotational constants and ground state molecular structure *(Dieke, (1934)).* The studying of broadband (˜A1A2 ← ˜X1A1) absorption of formaldehyde at high temperatures (67–1073 K) at 0.08MPa showed that, the photodissociation rat and spectral absorption coefficient have a strong dependence of temperature *(Mackey, (1997) Xiao (2004*))

Theory : .

1.1 Bessel functions of the first kind: Jm

The mathematical equation of Bessel function as follows:

$$x^2\frac{d^2y}{dx^2}+x\frac{dy}{dx}+(x^2\ -\ v^2)y=0.(1-a)$$

$J_m(x)$, is a solutions of Bessel's differential equation which is given by equation No.(1).

$$J_m(x)=\sum_{n=0}^{\infty}\frac{(-1)^n}{n!\ \Gamma\ (1+m+n)}\left(\frac{x}{2}\right)^{2n+m}\quad(1-b)$$

Where Γ (1+m+n) is the gamma function and J'_m is the first order derivative of J_m which is given by equation No.2:

$$J'_m(x)=\frac{x\,J_m(x)-m\,J_{m+1}}{x}\ldots..(2)$$

Similarly, higher order derivatives of $J_m(x)$ can be used to calculate the extended values of α_{mn} in the cylindrical cavity . The calculated new values of α_{mn} help us to understand the position of different types of excited acoustic modes in the cavity. It also

helps us to determine the common location or clustering of some of the excited modes at certain rang of frequencies.

1.2 Acoustic Modes

The frequency of acoustic resonant modes generated in the closed cylindrical cell is described by:

$$F_{mnq} = \frac{c}{2}\left((\frac{\propto_{mn}}{R})^2 + \left(\frac{q}{l}\right)^2 \right)^{\frac{1}{2}} \dots\dots\dots (3)$$

Where c is the sound velocity, α_{mn} is the nth zero of the derivative of the mth Bessel function at $r = R$, where R and L represent the radius and the length of the cylindrical cavity, respectively. The normal acoustic spectrum lines are separated into longitudinal (q), radial (n) and azimuthal (m) modes, respectively. The solution of the inhomogeneous wave equation of sound pressure in the cylindrical resonator provides three types of eigen function in the cavity. The first one is the longitudinal type and its frequency depends on the resonator length and can be calculated directly by:

$$F_{00q} = \frac{qc}{2l} \dots\dots\dots (4)$$

The form of the eigen function for the longitudinal type is given by:

$$P_n(r) = P_{00q}(z) = \cos(K_z z) \dots (5)$$

However, azimuthal and radial types are the other two modes which depend on the radius of the resonator and the jth zero of the derivative of the mth Bessel function divided by π. Their resonance frequencies can be ascertained by:

$$F_{mn0} = c\alpha' \frac{mn}{2\pi r} \dots\dots\dots (6)$$

And their corresponding eigen functions of mode distribution is given by:

$$P_n(r) = P_{mn0}(r, \emptyset) = J_m(K_r r)\{^{\cos(m\emptyset)}_{\sin(m\emptyset)}\} \dots (7)$$

Fig-4.2 shows the schematic of the acoustic longitudinal, azimuthal and radial modes produced in the cavity due to pulsed laser

1.3 Simulation of Acoustic modes distribution at higher frequency range:

The distribution of acoustic modes for Formaldehyde molecules in higher frequency range are calculated using equation no. (3). The corresponding theoretical values of α_{mn} are shown in table-1.

Table-1: the values of α_{mn} for m=3 and n=3

	m=0	m=1	m=2	m=3
n=1	5.33144	6.706133	8.015237	9.282396
n=2	8.536316	9.969468	11.34592	12.68191
n=3	11.706	13.17037	14.58585	15.96411
n=4	14.86359	16.34752	17.78875	19.19603

As per our experimental results, the theoretical values of the excited frequencies are restricted up to 40 kHz frequency range for all types of acoustic modes. Fig- 3 shows the dependency of acoustic mode distribution on Bessel function in the PA cell having dimension L=27cm and R=1.4cm .This figure is subdivided into four segments (I-IV). First segment shows 3 number of pure radial (RA), 5 numbers of pure azimuthal (AZ) and 40 numbers of pure longitudinal (LO) modes which occupies frequency range between 0-45kHz. The second segment shows the new mixed modes which is due to combinations of all these excited cavity modes along with pure modes .Similarly, the third segment shows the combined distribution of RA and LO modes. Here AZ=1 represents the zero value of an azimuthal mode.

2. Experimental set up

Fig.1 shows the schematic layout of experiment where λ=266 nm wavelength i.e. 4th harmonic of Q-switched Nd: YAG laser (Model Spit, Germany) is used to excite the Formaldehyde molecules in the PA cells. THIS cell IS made of stainless steel and designed and fabricated in the laboratory itself. Its internal diameter is 1.4 cm with average length of 27 cm, as shown in fig-2 . The PA signal is detected by a pre-polarized microphones having responsivity 50mV/Pa

. *Figure-2: Resonance cavity with filter(Length= 27cm & Radius =1.4cm (with a filter))*

Table-2: calculated longitudinal , radial and azimuthal modes

L1	**624**	**1250**	**1870**	**2500**	**3100**
L2	**3750**	**4365**	**5000**	**5610**	**6240**
RA	**7310**	**12130**	**16680**	**21120**	**25480**
AZ	**15220**	**27853**	**40410**	**52920**	**65.4422**

L=Longitudinal , RA= Radial & AZ=Azimuthal

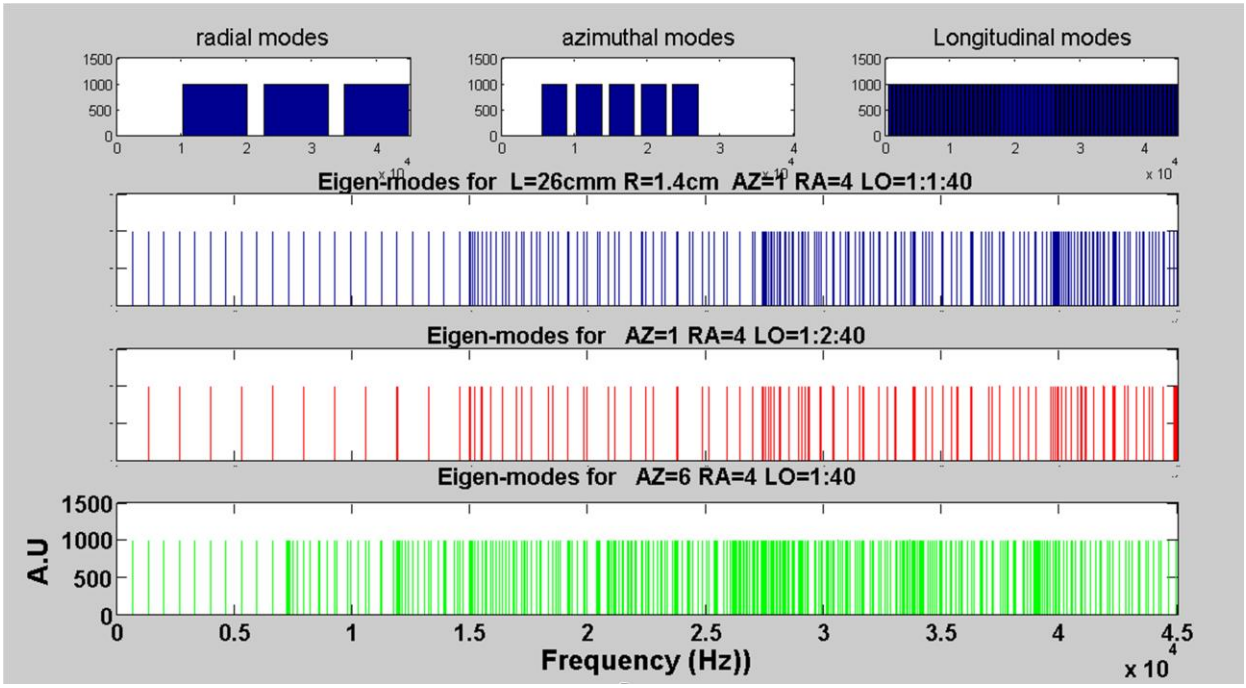

Figure-3: Simulation of resonance modes

(BSWA, China made). The microphone is placed in the center of the PA cell. The output signal of the microphone is fed to the preamplifier which is coupled to the 200 MHz Oscilloscope (Tektronix made in U.S.A.). The USB /GPIB interfacing is used for data acquisition through Boxcar integrator (Stanford Instruments Inc., USA made). The data analysis is done using software made in lab-view.

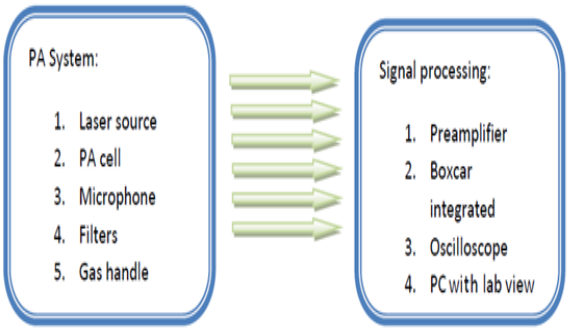

. *Figure (1) : Experimental setup*

3. Results and discussion

This part is divided to seven sections as follows: 1) Simulation part which deals with calculated resonance modes in the PA cavity and their theoretical distribution, 2) PA Spectrum of Formaldehyde deals with time and frequency PA spectrum of formaldehyde in the designed cavity, 3) The effect of input laser energy on PA Signal, 4) Effect of Pressure on PA Signal, 5) Quality-Factor of the resonance cell, 6) Effect of acquisition time on PA signal and 7) Low Limit of Detection of formaldehyde in N2 buffered.

3.1 Simulation part of theoretical excited modes inside resonance cavity :

In this section we have calculated the longitudinal , radial and azimuthal resonance frequencies inside the resonance cavity as listed in table -2 . The individual and complex longitudinal , radial and azimuthal have been simulated and presented in figure-3.

3.2 PA Spectrum of Formaldehyde

Fig-4 shows the PA signal in time domain and frequency domain using Fast Fourier transform FFT. The PA spectrum shows the clustering effect as a reflection part of the formaldehyde spectrum. The excited acoustic modes are appearing as two longitudinal acoustic modes which located at 3025Hz &3800 Hz, respectively. In addition, the second azimuthal mode is located at 27800Hz. The figure shows clearly the domination of longitudinal modes over radial and azimuthal modes. That is due to the additional in both sides coupled filter which increase the length of resonance cell. In fact the cell without filter is a radial dominator cavity while with filter it is a longitudinal dominator cavity.

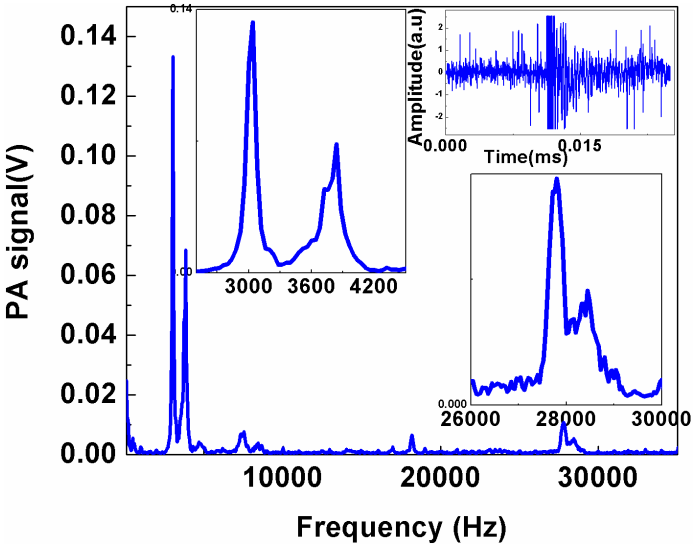

Figure(4): PA spectrum of Formaldehyde

Also, the figure show some small intensity excited modes which is related to radial modes. Such a modes can be observed clearly in the case of removing filters. However, formaldehyde has a good excited levels which has absorption near at 266nm.

Therefore, these levels appear as a closely modes in the acoustic form.

3.3 Effect of Input Laser Energy on PA Signal

The PA signal is recorded for formaldehyde molecules at different incident laser energy for both resonance modes as shown in fig- (6). The intensity of both longitudinal excited PA modes showed an exponential responding with incident laser energy.

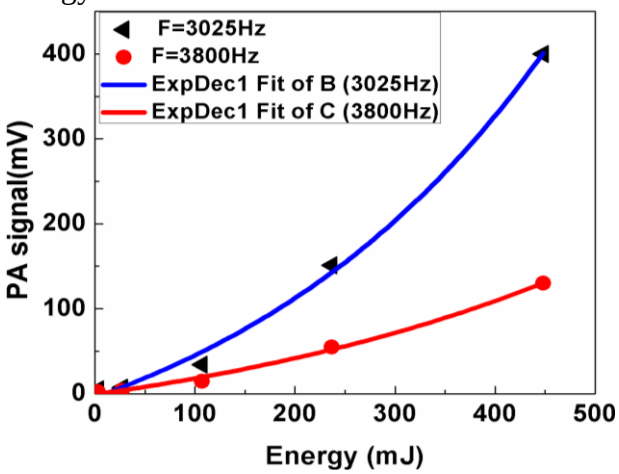

Figure-(6):Effect of laser energy on PA signal

The exponential variation of PA signal with respect to input laser energy at resonance frequency 3025 Hz showed highest stability over other excited modes 3800 Hz. The variation found in good agreement with ExpDec1 exponential equation:

$$PA\ signal = A\exp\left(\frac{-x}{t_1}\right) + Y_0 \ldots (8)$$

For the 5th longitudinal mode 3025Hz. the values of A=139.887 ± 64.96. t1=-329.32 ± 82.38 &Yo=-144.25 ± 71.8 and for the 6th longitudinal mode 3800Hz A=73.862 ± 39.5. t1=-438.75 ± 145.56, Yo=-74.65 ± 41.8.

3.4 Effect of Pressure on PA Signal

Figure-5 shows the variation of PA signal with formaldehyde pressure for the two longitudinal resonance frequencies 3025Hz &3800Hz, respectively. Both of them show a semi-linear increment with increases of formaldehyde pressure. However, at higher value of pressure the saturation effects start appearing for 5th longitudinal mode before 6th longitudinal mod.

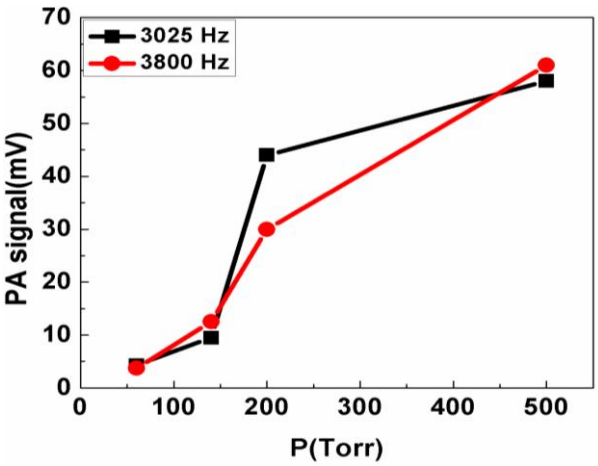

Figure-5 PA signal vs Sample pressure for two frequencies

3.5 Quality-Factor of the resonance cell

The value of quality factor reflects the quality or efficiency of the photo acoustic system. It depends on the efficiency of Photoacoustic resonance cavity. Physically, Quality factor defined as the ratio of the accumulated energy of resonance mode in one cycle to the energy lost over one cycle. It can be written mathematically as follows:

$$Q = \frac{2\pi\ accumulated\ energy}{energy\ lost\ over\ one\ period} = \frac{f0}{\Delta f} \ldots (9)$$

Where f_0 and Δf are the resonance frequency and the full width at half maximum of the resonance profile (FWHM)

Fig-7(a -c) shows the Lorentz fitting of the longitudinal and azimuthal intensity modes which located at 3025 Hz ,3800 Hz &27800Hz. It's very clear that, quality factor depends also on the order and type of the excited mode where the experimental estimating value of the quality factors of excited PA modes are 19, 35.6 & 77, respectively. The most interesting thing here is the highest value of q-factor for the azimuthal mode even the cell itself is a longitudinal cell. This results explained why most PA cavities are designed for excitation a radial and azimuthal modes.

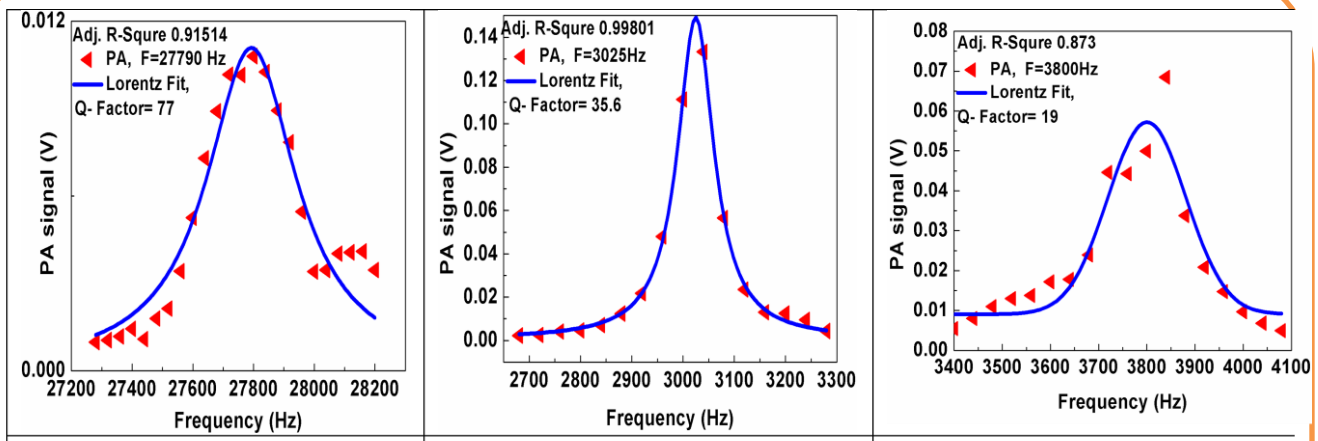

Q-factor with F=27790Hz | *Q-factor with F=3025Hz* | *Q-factor with F=3800Hz*

Figure(7): Lorentz fit of (a) 12.414 kHz (b) 22.713 kHz

3.6 Effect of acquisition time on PA signal:

In signal processing issue, the data acquisition system plays a very important role in the collection of all excited acoustic modes of different frequencies in different time scale frames.

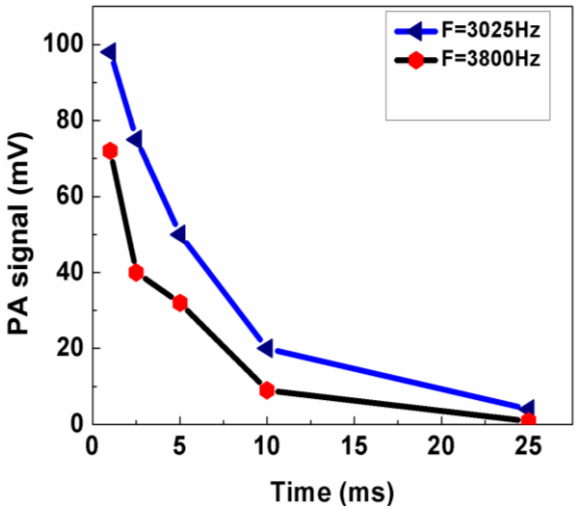

Figure(8): Time-based decay behavior of PA signals at 3025 kHz and 3800 kHz

For example, the PA spectrums for Formaldehyde in the resonance cavity as shown in fig-4 are recorded at acquisition time of 2.5ms which allows us to collect acoustic spectral lines up to 50 kHz. This also help us to identify the presence of some short life modes such as small intensity modes appeared at different frequencies. Fig-8 shows the behavior of Photoacoustic resonance modes at different acquisition times. It shows that, both excited frequencies are shown similar decay behavior with acquisition time.

3.7 Low Limit of Detection

The minimum detection limit of the designed PA systems can be calculated by calibration methods which depend on recording the PA signal at different concentration of the sample. At the linear response of the PA system, low limit of detection (S_{min}) is calculated by dividing the known concentration of the sample by the signal to noise ratio (SNR). We have recorded the background signal of the order of 0.18μV under similar experimental condition of pressure and laser energy. The typical strength of PA signal is recorded of formaldehyde at 1 Torr pressure buffered in air with total pressure 500 Torr. The low limit of detections of Formaldehyde buffered in air for both PA modes is reported in table-1 along with other important parameters.

Table-3: Important parameters

Mode/Parameters	F(Hz)	Q	*Smin*(ppbV)
5thLong.	3050	35.6	3.6

4. Conclusion

We have successfully recorded the photoacoustic signal in time and frequency domains for formaldehyde in special designed resonance PA cell. The systematic study of dependency of PA signals with respect to incident input laser energy, formaldehyde pressure and acquiescing time has also been carried out along with comparative study of quality factor of all excited resonance PA modes. This improvised design helps us to achieve minimum limit of detection (S_{min}) of formaldehyde according to strong mode is 3.6 ppbV.

5. References

1. Sigrist, W.M. (1994) *Air Monitoring by Spectroscopic Techniques*, New York: John Wiley and Sons.
2. Yehya, F. (2011) "Designing and Modeling of Efficient Resonant Photo Acoustic Sensors for Spectroscopic Applications," J. Mod. Phys., vol. 2, no. 4, pp. 200–209.
3. Sigrist, M. W. .et al (2001) "Environmental Spectroscopy Applications of Photoacoustic," Anal. Chem., vol. 17, pp. 511–514.
4. Thöny, A. and Sigrist, M. W. (1995) "New developments in CO2-laser photoacoustic monitoring of trace gases," Infrared Phys. Technol., vol. 36, no. 2, pp. 585–615, 1995.
5. Sigrist, W. M. (1994) In Air Monitoring by Spectroscopic Techniques. New York: John Wiley & Sons, Inc.
6. Miklós, A. Hess, P. and Bozóki, Z . (2001) "Application of acoustic resonators in photoacoustic trace gas analysis and metrology," Rev. Sci. Instrum., vol. 72, no. 4, pp. 1937–1955.
7. Slezak, V. Santiago, G. and Peuriot, A. L. (2003) "Photoacoustic detection of NO2 traces with CW and pulsed green lasers," Opt. Lasers Eng., vol. 40, no. 1–2, pp. 33–41.
8. Harren, F. J. M. ..et al(2000) "Photoacoustic Spectroscopy in Trace Gas Monitoring," Encycl. Anal. Chem., pp. 2203–2226.
9. Schäfer, S. Mashni, M. Sneider, J. and Mikl, A. (1998) "Sensitive detection of methane with a 1 . 65 µ m diode laser by photoacoustic and absorption spectroscopy," Appl. Phys. B, vol. 66, pp. 511–516.
10. Yehya, F. and Chaudhary, A. K. (2013) "Time resolved high frequency spectrum of Br2 molecules using pulsed photoacoustic technique.," Spectrochim. Acta. A. Mol. Biomol. Spectrosc., vol. 115, pp. 544–51.
11. Yehya, F. and Chaudhary, A. K. (2014) "Study of damping, saturation and surface losses on low level detection of NO2 using time resolved pulsed photo acoustic technique," Opt. Commun., vol. 312, no. 2, pp. 16–22
12. Rao, K. S. Yehya, F. Chaudhary, A. K. Kumar, A. S. and Sahoo, A. K. (2014) "Thermal Stability Study of Nitro-rich Triazole Derivatives using Temperature dependent Time resolved Pulsed Photoacoustic (PA) Technique," J. Anal. Appl. Pyrolysis, vol. 109, 2, 132–139,
13. Rao, K. S. and Chaudhary, A. K. (2017) "Comparative Study of Ultraviolet Laser-Based Time-Resolved Photoacoustic Fingerprint Spectra and Thermal Decomposition Mechanisms of Energetic 1,2,3-1H-Triazole Derivatives Under Controlled Pyrolysis," Appl. Spectrosc., vol. 71, no. 7, pp. 1–13.
14. Angelmahr, M (2006). Photoacoustic spectroscopy of formaldehyde with tunable laser radiation at the parts per billion level Appl. Phys. B 85, 285–288 .
15. Davenport J (2014) UV Spectroscopic Instrumentation for Formaldehyde Detection in the Indoor Environment PhD Thesis, School of Engineering , Cranfield University, January 2014
16. Brasseur P, Orlando JJ, Tyndall GS. (1999) Atmospheric chemistry and global Change. Oxford University Press; 1999

17. Adewuyi, Y.G, et al (1984) Importance of formaldehyde in cloud chemistry, Atmos. Environ. 1967. 18 , 2413–2420.
18. Anderson, L.G. et al (1996) Sources and sinks of formaldehyde and acetaldehyde: An analysis of Denver's ambient concentration data, Atmos. Environ. 30 , 2113–2123.
19. Hak, C. et al., (2005) Intercomparison of four different in-situ techniques for ambient formaldehyde measurements in urban air, Atmos. Chem. Phys. 5 2881–2900.
20. Committee on Sick House Syndrome: Indoor Air Pollution Progress Report.No. 4, Japan., (2002).
21. Ebeler, S.E. et al (1997) , Quantitative analysis by gas chromatography of volatile carbonyl compounds in expired air from mice and human, J. Chromatogr. B. Biomed. Sci. App. 702 , 211–215.
22. Lu Y, Liu J, Lu B, Jiang A and Wan C(2010) Study on the removal of indoor VOCs using miotechnology J. Hazardous Mater. 182 204–9
23. Kim S (2010) Control of formaldehyde and TVOC emission from wood-based flooring composites at various manufacturing processes by surface finishing J. Hazardous Mater. 176 14–19
24. Nielsen G D and Wolkoff P (2010) Cancer effects of formaldehyde: a proposal for an indoor air guideline value Arch. Toxicol. 84 423–46